Multi-step magnetic ordering in frustrated thiospinel $MnSc_2S_4$

2007 J. Phys.: Condens. Matter 19 145262

(http://iopscience.iop.org/0953-8984/19/14/145262)

IOP PUBLISHING JOURNAL OF PHYSICS: CONDENSED MATTER

J. Phys.: Condens. Matter **19** (2007) 145262 (6pp) doi:10.1088/0953-8984/19/14/145262

Multi-step magnetic ordering in frustrated thiospinel $MnSc_2S_4$

M Mücksch[1,2], M M Koza[2], H Mutka[2], C Ritter[2], A Cervellino[3], A Podlesnyak[3], D Sheptyakov[3], V Tsurkan[1,4], A Krimmel[1], S Horn[1] and A Loidl[1]

[1] Institut für Physik, Universität Augsburg, D-86135 Augsburg, Germany
[2] Institute Laue Langevin, BP156 X, F-38042 Grenoble Cedex 9, France
[3] Laboratory for Neutron Scattering, PSI Villigen & ETH Zürich, CH-5232 Villigen, Switzerland
[4] Institute of Applied Physics of the Moldova Academy of Sciences, MD-2028 Chisinau, Republic of Moldova

E-mail: michael.muecksch@physik.uni-augsburg.de

Received 31 August 2006
Published 23 March 2007
Online at stacks.iop.org/JPhysCM/19/145262

Abstract

Energy resolved neutron diffraction elucidates the magnetic ordering process in the magnetic A-site thiospinel compound $MnSc_2S_4$, which reveals two magnetic transitions at $T_{N1} = 2.3$ K and $T_{N2} \simeq 1.9$ K. The coexistence of long range magnetic order and remaining short range contributions with different propagation vectors for $T_{N2} \simeq 1.9\ \text{K} \leqslant T \leqslant 2.3\ \text{K} = T_{N1}$ clarifies that the transition at $T_{N2} \simeq 1.9$ K is first order. The ordering process can be described in the framework of single- and double-**q** short range order fluctuations around $\mathbf{q} \cong (100)$ approaching the magnetic ordering transition at $T_{N1} = 2.3$ K from the high temperature paramagnetic state. The double-**q** short range contribution may serve as a precursor for the finally stabilized spiral structure with $\mathbf{q} \cong (\frac{3}{4}\frac{3}{4}0)$ for $T \lesssim T_{N1}$. Anisotropic magneto-elastic coupling is suggested to induce the magnetic ordering and to lift a possible exchange frustration via an associated lattice distortion.

(Some figures in this article are in colour only in the electronic version)

1. Introduction

The current interest in frustrated magnetic systems (see e.g. [1]) is linked to the formation of new exotic ground states and the wish to obtain deeper insight into the microscopic 'quantum' driving forces, which are responsible for establishing macroscopically long range ordered states or for suppressing them. Most often additional contributions like magnetic anisotropy, dipole–dipole interactions or spin–lattice coupling may lift the geometric and/or exchange frustration and lead to a long range ordered ground state. A model system for the suppression of magnetic order well below the mean field Curie–Weiss temperature θ_{CW} are the normal spinel compounds

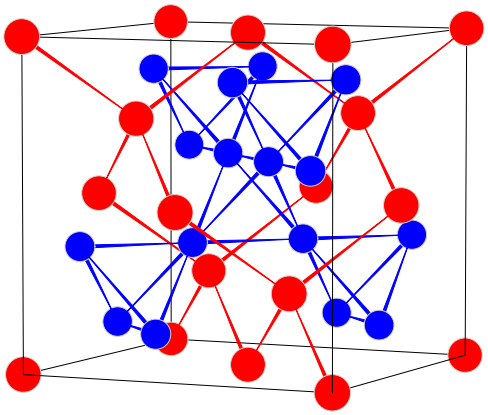

Figure 1. Unit cell of the spinel structure with the A sublattice network in grey (red) and the corner sharing tetrahedral B sublattice network in black (blue).

MSc_2S_4 (M = Fe, Mn) [2, 3]. The magnetic M^{2+} ions are only located on the crystallographic A sites, whereas the B sites are occupied by nonmagnetic ($3d^0$) Sc^{3+} ions. The structure for A and B sites is illustrated in figure 1. $FeSc_2S_4$ with a Curie–Weiss temperature $\theta_{CW} = -45$ K remains paramagnetic down to 50 mK, leading to a frustration parameter $f = |\theta_{CW}|/T_N \gtrsim 900$, and reveals a spin–orbit liquid ground state [2, 4]. $MnSc_2S_4$ with Mn^{2+} ions in a principal spin-only $3d^5$ ($S = 5/2$) state and a lattice parameter $a = 10.599$ Å ($T = 1.5$ K) exhibits a Curie–Weiss temperature of $\theta_{CW} \cong -22$ K [2, 5]. A magnetic ordering process takes place in the form of two subsequent transitions at $T_{N1} = 2.3$ K and $T_{N2} \simeq 1.9$ K, corresponding to a frustration parameter $f \simeq 10$ [2]. The specific heat shows that only 30% of the total expected magnetic entropy is recovered at the first phase transition T_{N1} and the full magnetic entropy is recovered only around $T \sim 20$ K [2]. This is consistent with deviations from the Curie–Weiss law and the observation of magnetic diffuse neutron scattering for $T \lesssim |\Theta_{CW}|$ [5]. The two subsequent phase transitions are observed in neutron scattering, magnetization and specific heat experiments [2] and were discussed in [5] as magnetic and possibly crystallographic in origin. The magnetic ground state structure below $T_{N2} \simeq 1.9$ K with a propagation vector $\mathbf{q} \cong (0.75, 0.75, 0)$ violates the cubic crystal symmetry [5], consistent with NMR results [6, 7]. We now further discuss the unusual and complex magnetic ordering process by a detailed study of the energy resolved diffuse magnetic scattering in the vicinity of the magnetic phase transitions and additional low temperature neutron diffraction.

2. Experiment

Experiments were performed on polycrystalline powder samples used already in previous studies [5] at the cold neutron time-focusing time-of-flight spectrometer IN6 at the Institute Laue–Langevin in Grenoble (France) and with a comparable setting at the cold neutron time-of-flight spectrometer FOCUS at the Paul Scherrer Institute in Villigen (Switzerland) in the temperature range of $1.45 \leqslant T \leqslant 5$ K. The incident neutron wavelength of 5.9 Å at both spectrometers results in a resolution limited elastic energy linewidth of 50 μeV. The time-of-flight data were treated with the LAMP program suite [8] in a standard way, i.e. were converted to $S(Q, \omega)$ after correction for background and normalization with respect to a standard vanadium sample measured under comparable conditions. Additionally, neutron powder diffraction experiments were carried out at the cold neutron diffractometer DMC at the Paul Scherrer Institute, Villigen (Switzerland) with a He^3/He^4 dilution cryostat in a temperature range 120 mK $\leqslant T \leqslant$ 2.2 K with an incident neutron wavelength of 2.45 Å.

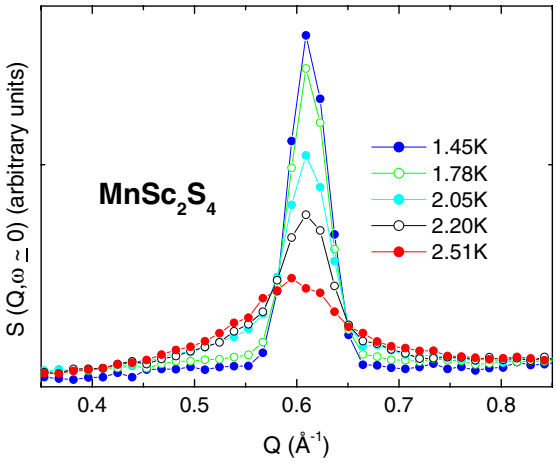

Figure 2. Temperature dependent elastically resolved intensity measured on FOCUS. For clarity the error bars have been suppressed.

The data were collected for several detector bank positions with an angular step of 0.1°. All data were normalized on a monitor and the 2θ dependence was transformed to a $Q = 4\pi \sin(2\theta/2)\lambda^{-1}$ dependence for ease of comparison.

3. Results and discussion

Neutron diffraction is an energy integrative measurement, i.e. a 2θ dependent sum over static and dynamic contributions. The separation of the static and dynamic scattering contributions by use of energy selective techniques is required for a proper characterization of a phase transition, since much of the signal is dynamic in origin. These dynamic fluctuations can mask the diffraction pattern, as has been pointed out previously [5]. Neutron time-of-flight spectroscopy measures the dynamic scattering function $S(Q, \omega)$ and the data analysis allows us to separate the zero energy transfer contribution $S(Q, \omega \simeq 0)$ limited only by the instrumental resolution. $S(Q, \omega \simeq 0)$ provides unique information about the structure evolution, as $S(Q, \omega = 0)$ represents in real space the true static long time average structural components.

An impression of the phase transitions in $MnSc_2S_4$ is given by the elastically resolved FOCUS data presented in figure 2. The first remarkable feature evident from figure 2 is the asymmetric magnetic diffuse scattering around the magnetic long range order reflection at $Q = 0.628$ Å^{-1} corresponding to the (0.75, 0.75, 0) reciprocal lattice position. Looking more precisely at the region of the strongest magnetic reflection around $Q = 0.6$ Å^{-1}, we see in figure 2 a broad distributed intensity for $T = 2.5$ K $> T_{N1} \simeq 2.3$ K, representing short range ordering, as also found in the previous diffraction and time-of-flight spectroscopic studies [5]. With the new FOCUS data we are now able to separate elastic and dynamic contributions in the region $T_{N2} < T < T_{N1}$, which was previously not covered by the energy resolving time-of-flight measurements at IN6. $S(Q, \omega \simeq 0)$ for this temperature range (see figure 2) indicates a coexistence of a remaining broad short range order contribution and the evolving long range order structure peak at (0.75, 0.75, 0). The centre of the short range order intensity can be attributed to a (100) propagation, which is different from the final magnetic propagation direction and modulus. Below the second phase transition at $T_{N2} \simeq 1.9$ K we observe essentially the long range order contribution only.

To quantify this behaviour we fitted $S(Q, \omega \simeq 0)$ for the strongest magnetic reflection around $Q = 0.6$ Å^{-1} with two Gaussian lines corresponding essentially to a (100) and a (0.75,

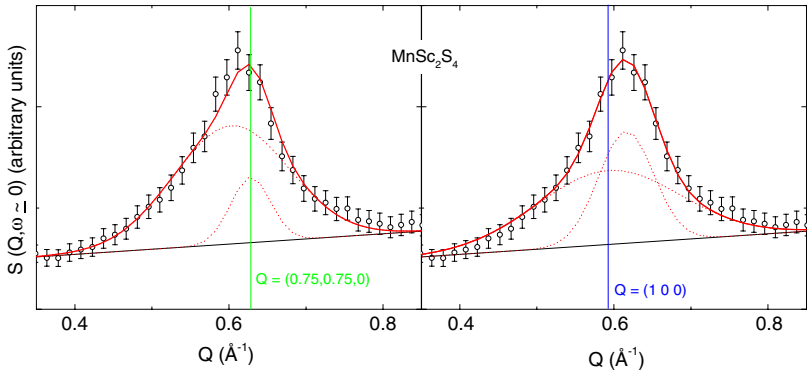

Figure 3. Exemplary fits of the of $S(Q, \omega \simeq 0, T = 2.5$ K) (solid line) by two Gaussian lines (dotted lines). The position of one of the Gaussian peaks was fixed at either $Q = (0.75, 0.75, 0)$ (left frame) or $Q = (100)$ (right frame), indicated by the vertical lines.

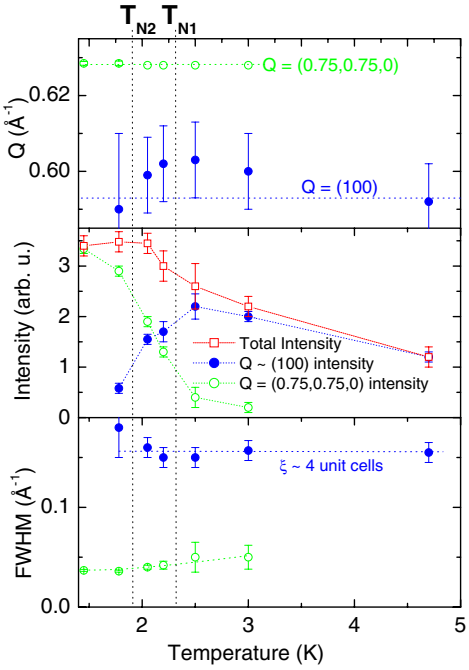

Figure 4. Results of the fitting procedure as described in the text. Temperature dependent peak positions are in the upper frame, peak intensities are in the middle frame and peak widths are in the lower frame. The dotted lines are a guide for the eye with the vertical lines indicating T_{N1} and T_{N2}, respectively.

0.75, 0) propagation. Figure 3 shows exemplary results, fixing one Gaussian centre either at the (100) reciprocal lattice position ($Q = 0.593$ Å^{-1}) or at the (0.75, 0.75, 0) reciprocal lattice position ($Q = 0.628$ Å^{-1}). Figure 4 summarizes the results of the model with fixed (0.75, 0.75, 0) centre position to reflect the evolution of long range order. Essentially for $T \leqslant T_{N1}$ there is no significant difference between the two models. The long range order peak position is well defined by the sharp Bragg reflection at $Q = 0.628$ Å^{-1}, whereas the short range centre position due to its rather broad nature is less accurately defined around a Q position equivalent to the (100) reciprocal lattice position. Consequently, a fixing of the (100) contribution at $Q = 0.593$ Å^{-1} neither affects significantly the quality of the fit nor the resulting intensities in

this temperature range. Independently of the chosen fit model, there is a significant difference between the fitted short range order and long range order centre positions (figure 4 upper frame), as indicated already above in figure 2 by the peak asymmetry. For $T > T_{N1} = 2.3$ K the fitting process is less evident as illustrated in figure 3. The model with the fixed (100) centre position seems to be slightly better than the model with the fixed (0.75, 0.75, 0) centre position. This may reflect a slight deviation of the magnetic propagation above the first magnetic ordering temperature $T \gtrsim T_{N1}$ from the (0.75, 0.75, 0) to an incommensurate value. For the 5 K data the fitting results effectively in only one Gaussian with a centre position corresponding to the (100) position, thus there is no (0.75, 0.75, 0) contribution remaining. The evolution of the intensity of the two contributions is illustrated in the middle frame of figure 4. At 5 K we only have the short range order contribution. On cooling, the growing long range order contribution is accompanied by a decreasing short range order contribution, which completely vanishes for $T = 1.45$ K. The total ordered intensity as a sum of both contributions steadily increases. In the lower frame of figure 4 we see that the full width at half maximum (FWHM) of the (100) contribution remains unchanged for $T_{N2} \leqslant T \leqslant 5$ K. This FWHM corresponds to a measure of a correlation length $\xi \simeq 2\pi/\text{FWHM}$ of about four unit cells, i.e. the correlations with a (100) propagation are always in the spatial range of the ground state magnetic unit cell. The FWHM of the long range magnetic order contribution approaching T_{N1} on cooling reflects correlations over at least eight unit cells. For $T \lesssim T_{N2}$ this width is comparable to the (111) nuclear peak width, indicating full long range order.

The magnetic structure with a propagation vector $\mathbf{q}$ generates reflections for $(hkl) \pm \mathbf{q}$. Thus the first observed reflection consists of a (000) + $\mathbf{q}$ and (111) − $\mathbf{q}$ contribution. This reflection would split if $\mathbf{q} \neq (0.75, 0.75, 0)$. However, the positions of the two short range order contributions around (0.75, 0.75, 0) and (100) are incompatible with such a splitting. This evidences the coexistence of two emerging different kinds of diffuse magnetic contributions above T_{N2}, indicating two energetically close kinds of structure states, possibly due to exchange frustration. The long range order develops around $Q \simeq 0.62$ Å^{-1} and the other contribution centred at the (100) reciprocal lattice position is completely suppressed below T_{N2}.

The (100) reciprocal lattice position indicates antiferromagnetic (AFM) correlations according to a type-I AFM structure (see e.g. [9]). Normally, such structures are single-**q** valued. A double-**q** structure is energetically equivalent to a single-**q** structure, but probably stabilized by strong magneto-crystalline anisotropy along the (110) crystal direction [9]. In such a situation the double-**q** structure can coexist in competition with the collinear single-**q** structure by combining two different single-**q** propagations like e.g. (100) + (010) resulting in alternating FM planes perpendicular to the (110) direction. Normally, there is no chance to distinguish such a single-**q**/double-**q** structure, since both contributions exhibit identical periodicity [9]. Additionally, the formation of the final spiral structure below T_{N2} (compared to a collinear single-**q** structure along (100)) indicates the presence of anisotropy, as the spiral structure type is stabilized compared to a collinear structure in case of anisotropic interactions [9]. Therefore, a possible interpretation of the magnetic diffuse scattering ($T > T_{N1}$) around $Q \simeq 0.62$ Å^{-1} could be fluctuations of double-**q** type, as this kind of structure is similar to the magnetic ground state spiral structure, which also alternates along the (110) direction. Such a type of double-**q**-like fluctuations may have a slightly deviating **q** value approaching T_{N1} compared to the (100) position most possibly due to spin–lattice coupling. This means that the magnetic ordering starts from a principal $\mathbf{q} = (100)$ propagation consisting most probably of single-**q** and double-**q** contributions, which transform on cooling by anisotropic magneto-elastic coupling via an additional incommensurate double-**q**-like contribution for $T > T_{N1}$ to the finally stabilized spiral with a propagation $q \cong (0.75, 0.75, 0)$ below T_{N2} suppressing the original target structure.

The magnetic structure of $MnSc_2S_4$ at low temperatures was further studied at the instrument DMC in a temperature range 120 mK $\leqslant T \leqslant$ 2.2 K. As a result we find no positional changes of the magnetic reflections, but the intensities increase due to freezing out of spin-wave excitations. The data were treated with the Rietveld method using the program FullProf [10]. The obtained propagation vector is within the accuracy of the measurement $q \cong (0.75, 0.75, 0)$ commensurable for the cubic symmetry, but a slight deviation from the cubic structural propagation to an incommensurate value due to a probable lattice distortion is not excluded. A fit of the low temperature dependent magnetic moment as obtained by the Rietveld refinement with a Bloch function $M(T) = M_0 * (1 - \text{const} * T^{\alpha})$ with M_0 the magnetization at zero temperature and α the exponent of the Bloch function results in a magnetic moment $M_0 = 4.7(1)\mu_B$ and an exponent $\alpha = 2.0(5)$. The value of zero magnetic moment M_0 is slightly reduced compared to the expected 5 μ_B of Mn^{2+}. This may be explained by crystal imperfections or a reduction via an orbital contribution due to spin–lattice coupling.

4. Conclusion

We evidence a quite unusual and complex phase transition behaviour of $MnSc_2S_4$. Furthermore, we find by use of the elastically resolved $S(Q, \omega \simeq 0)$ two different kinds of magnetic short range fluctuations for $T \geqslant T_{N1}$ indicating two energetically almost degenerate thermodynamic states maybe due to competing exchange interactions, which would result in different structures. For $T_{N2} \simeq 1.9$ K $\leqslant T \leqslant 2.3$ K $= T_{N1}$ we resolved the coexistence of short and long range order contributions with different propagation vectors, which evidences that the nature of the lower phase transition is essentially first order. The development of the magnetic order can be described in the framework of single/double-**q** short range order fluctuations, which transform via a non-collinear double-**q**-like incommensurate propagation to the long range ordered ground state spiral structure by magneto-crystalline anisotropy and/or anisotropic interactions combined with spin–lattice coupling. This magnetic ordering violates the cubic spinel symmetry and therefore the degeneracy due to possible exchange frustration may be lifted by some lattice distortion.

Acknowledgments

Experiments were partly performed at the Swiss neutron source SINQ and assisted by the Sample Environment and Polarized Targets groups of LDM at PSI, Villigen, Switzerland. This work was supported by the DFG via SFB 484, Augsburg.

References

[1] Ramirez A P 2001 *Handbook of Magnetic Materials* vol 13, ed K H J Buschow (Amsterdam: Elsevier Science) p 423
[2] Fritsch V, Hemberger J, Büttgen N, Scheidt E W, Krug von Nidda H A, Loidl A and Tsurkan V 2004 *Phys. Rev. Lett.* **92** 116401
[3] Reil S, Stork H-J and Haeuseler H 2002 *J. Alloys Compounds* **334** 92
[4] Krimmel A, Mücksch M, Tsurkan V, Koza M M, Mutka H and Loidl A 2005 *Phys. Rev. Lett.* **94** 237402
[5] Krimmel A, Mücksch M, Tsurkan V, Koza M M, Mutka H, Ritter C, Sheptyakov D V, Horn S and Loidl A 2006 *Phys. Rev.* B **73** 014413
[6] Giri S, Nakamura H and Kohara T 2005 *Phys. Rev.* B **72** 132404
[7] Büttgen N, Zymara A, Kegler C, Tsurkan V and Loidl A 2006 *Phys. Rev.* B **73** 132409
[8] http://www.ill.fr/data_treatment/lamp/front.html
[9] Rossat-Mignod J 1987 *Methods in Experimental Physics* vol 23C, ed K Sköld and D L Price (Orlando-London: Academic) p 69
[10] Rodríguez-Carvajal J 1993 *Physica* B **192** 55